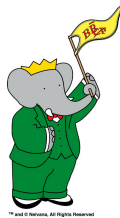


Angular analysis of $\overline{B} \rightarrow D^{(*)}\ell^-\bar{\nu}_\ell$ with hadronic tagging at *BaBar*

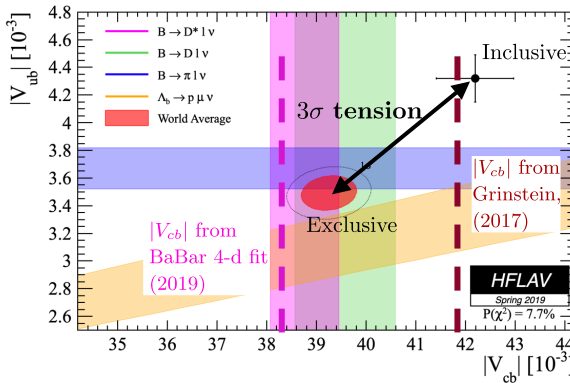
Biplab Dey

(on behalf of the BaBar Collaboration)

ICHEP, Bologna, 2022



$|V_{ub}|-|V_{cb}|$: TENSIONS IN TWO CRITICAL PARAMETERS

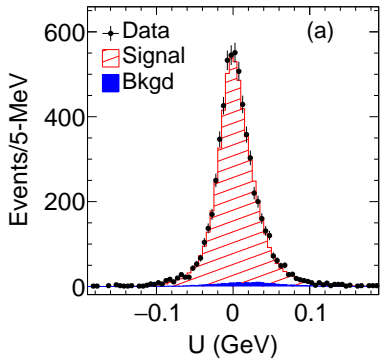


- Circa 2017, Grinstein/ Gambino: $|V_{cb}|$ “resolved” by zero-recoil extrapolation issue?
- 2019: back to the drawing board.
- 2021/22: lattice $w > 1$ FF’s.

- Note: some tension in $|V_{cb}|$ between $B \rightarrow D^*$ and $B \rightarrow D$.
- Stress-testing HQET and flavor-SU(3) ($B \rightarrow D^{(*)}$ vs $B_s \rightarrow D_s^{(*)}$).
- Implications of the form-factors on SL LFUV.

RECAP OF BABAR-19 $B \rightarrow D^*$ PAPER [PRL123, 091801 (2019)]

- First full 4-d $\overline{B} \rightarrow D^* \ell^- \bar{\nu}_\ell$ angular analysis with hadronic tagging.
- Single missing neutrino fully reconstructed ($U = E_\nu - p_\nu$).



- Extremely clean. Percent level resolutions in angular variables.
- ~ 6000 signal events. $N = 2$ (linear) BGL ([hep-ph/9508211](#)) fit adequate.
- Negligible effect on extracted $|V_{cb}|$ between BGL and CLN FF parameterisations.

HQET FF's AND THE RATIO OBSERVABLES

- H_λ amplitudes are written in terms of four form-factors.
- HQET: FF's only depend on w , the gamma-factor between B and recoiling D^* .

$$\frac{\langle D^*(v', \varepsilon) | V^\mu | \bar{B}(v) \rangle}{\sqrt{m_B m_{D^*}}} = i \textcolor{red}{h_V}(w) \epsilon^{\mu\nu\alpha\beta} \varepsilon_\nu^* v'_\alpha v_\beta$$

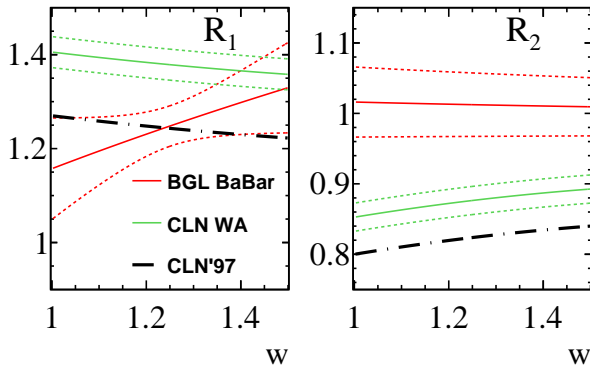
$$A_1 = \frac{w+1}{2} r' \textcolor{red}{h}_{A_1}$$

$$\begin{aligned} \frac{\langle D^*(v', \varepsilon) | A^\mu | \bar{B}(v) \rangle}{\sqrt{m_B m_{D^*}}} &= \textcolor{red}{h}_{A_1}(w)(w+1)\varepsilon^{*\mu} - \textcolor{red}{h}_{A_2}(w)(\varepsilon^* \cdot v)v^\mu \\ &\quad - \textcolor{red}{h}_{A_3}(w)(\varepsilon^* \cdot v)v'^\mu \end{aligned}$$

$$\begin{aligned} A_2 &= \frac{r h_{A_2} + h_{A_3}}{r'} \equiv \frac{\textcolor{blue}{R}_1 \textcolor{red}{h}_{A_1}}{r'} \\ V &= \frac{h_V}{r'} \equiv \frac{\textcolor{blue}{R}_1 \textcolor{red}{h}_{A_1}}{r'} \end{aligned}$$

- HQS limit: $\{h_V, h_{A_1}, h_{A_3}\} \rightarrow \zeta(w)$ and $h_{A_2} \rightarrow 0$.
- The two ratio observables $\textcolor{blue}{R}_{1,2}$ have reduced hadronic uncertainties.
- BGL basis $\{f_0, F_1, g, F_2\}$: rewrites h_{V,A_1,A_2,A_3} .

BABAR-19: DEVIATIONS IN $R_{1,2}$



- Figure as is, from the *BABAR-19* paper using BGL fits.
- “CLN-WA” used HFLAV16 numbers.
- CLN’97: original paper w/o uncertainties.

$R_{1,2}$ CONUNDRUM (CONTD.)

- $R_1(1)$ moved from 1.404 ± 0.032 (HFLAV16) to 1.269 ± 0.026 (HFLAV21, *BABAR-19* not included). Almost 3.3σ change! Latest number is close to *BABAR-19*.
- Experimentally, needs to be resolved: $R_2(1) \sim [h_{A_2}, h_{A_3}]/h_{A_1}$. HFLAV21 (excluding *BABAR-19*) quotes $R_2(1) \sim 0.85$.

FURTHER DEVELOPMENTS: LATTICE $w > 1$ DATA

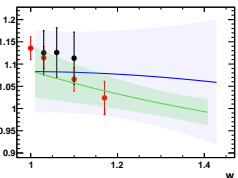
- Significant inputs from lattice now in $w > 1$ for $B \rightarrow D^*$. Independent validations of FFs.
- FNAL/MILC and JLQCD ($B \rightarrow D^*$) and HPQCD ($B_s^0 \rightarrow D_s^*$, full q^2). Lots of checks possible.
- Checks for flavor SU(3) in $B_{(s)} \rightarrow D_{(s)}^*$. Include BABAR $B \rightarrow D$ data.
- Goal: joint $B \rightarrow D^{(*)}$ HQET fits including all information, to interpret the FFs.
- Caveat: *everything shown today is preliminary.*

$B \rightarrow D^*$ BABAR + LATTICE FITS: SETUP

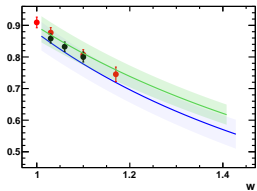
- Dataset remains the same as in BABAR-19 paper ($N_{\text{sig}} \sim 6000$).
- Main change is access to $N = 3$ BGL expansion due to including the new lattice $w > 1$ data w/o breaking unitarity conditions.
- $\{3, 3, 3, 2\}$ z expansion configuration for BGL basis $\{f_0, F_1, g, F_2\}$.
- F_2 is least constrained. Lattice-only.
- Try various combinations of BABAR + lattice:
 - BaBar+lattice fit result is in green.
 - HPQCD data is blue
 - FNAL/MILC data is red.
 - JLQCD data is black.
- HPQCD $B_s \rightarrow D_s^*$ FF converted to $B \rightarrow D^*$ using flavor SU3.

BaBar + HPQCD [FNAL/MILC, JLQCD]

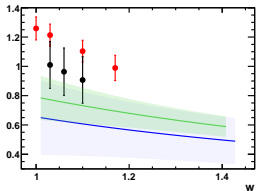
R_0 :



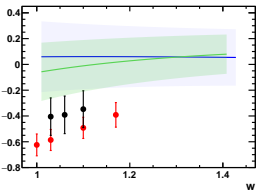
h_{A_1} :



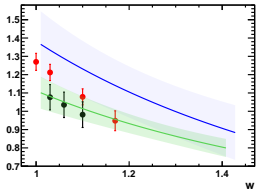
h_{A_3} :



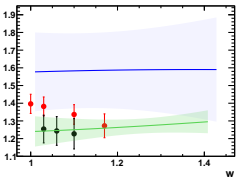
h_{A_2} :



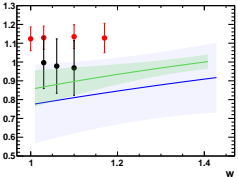
h_V :



R_1 :

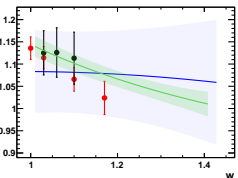


R_2 :

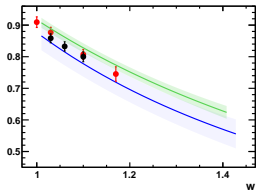


BaBar + FNAL/MILC [HPQCD, JLQCD]

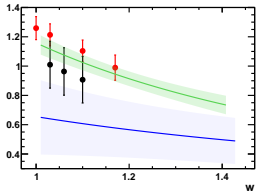
R_0 :



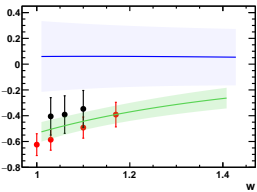
h_{A_1} :



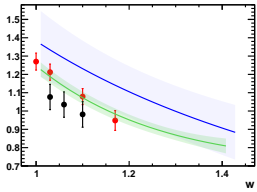
h_{A_3} :



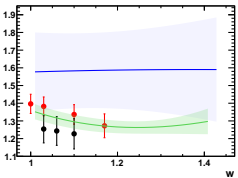
h_{A_2} :



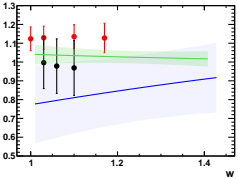
h_V :



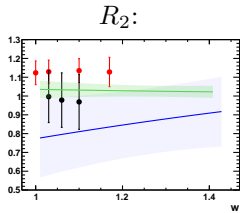
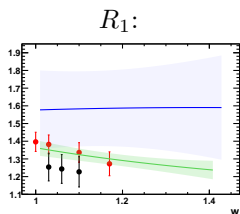
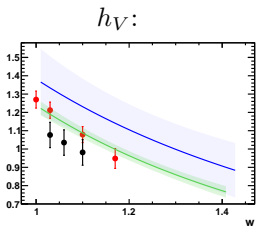
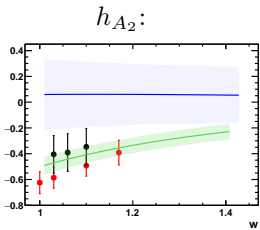
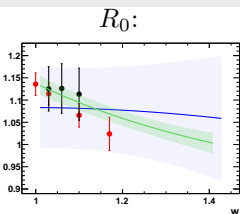
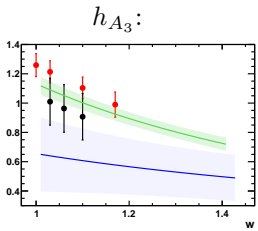
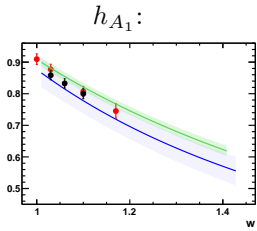
R_1 :



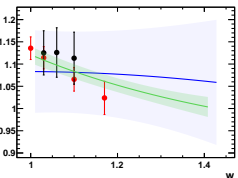
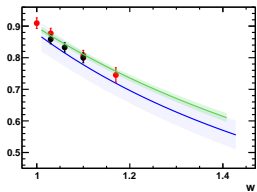
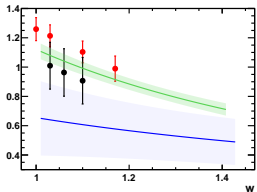
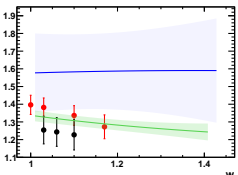
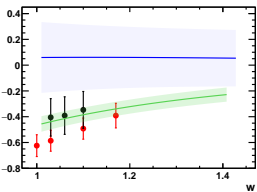
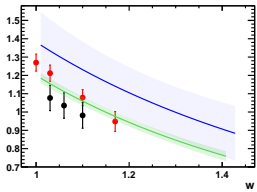
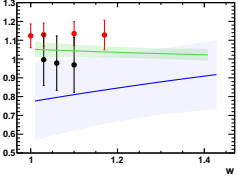
R_2 :



BaBar + FNAL/MILC + HPQCD [JLQCD]



BaBar + FNAL/MILC + HPQCD + JLQCD

 $R_0:$  $h_{A_1}:$  $h_{A_3}:$  $R_1:$  $h_{A_2}:$  $h_V:$  $R_2:$ 

TAKEAWAYS: FORM-FACTORS

- Adding three new independent **lattice** data over the past two years **did not change** the overall conclusions in **BABAR-2019** paper.
- Especially true in the “clean” ratio observables $R_{1,2}$.
- Some movement among different lattice calculations.
- HPQCD errors are largest and trends show some deviations from **BABAR +FNAL/MILC+JLQCD**. **Flavor SU3 violation** for $B \rightarrow D^*$?
- These combined fits are most precise, and also **robust** (no funny instabilities).

FIT QUALITIES

Type	<i>BABAR</i> NLL	MILC χ^2	HPQCD χ^2	JLQCD χ^2
HPQCD	103441	69.7	3.6	25.1
MILC+JLQCD	103441	14.2	20.2	5.7
ALL	103443	13.1	8.0	5.9

- Also FNAL/MILC uncertainties as provided are smallest.
- Overall, *BABAR* can accommodate the new lattice data ($\chi^2/\text{ndf} < 1$) quite well.

EFFECT OF LATTICE ON $|V_{cb}|$

- Use HFLAV-16 $B \rightarrow D^*$ BFs, but include all lattice data now.
- $|V_{cb}| \times 10^3$ moves from 38.36 ± 0.90 to 38.93 ± 0.68 . *Not* sensitive to zero-recoil extrapolation.

EFFECT OF LATTICE ON $|V_{cb}|$

- Use HFLAV-16 $B \rightarrow D^*$ BFs, but include all lattice data now.
- $|V_{cb}| \times 10^3$ moves from 38.36 ± 0.90 to 38.93 ± 0.68 . *Not* sensitive to zero-recoil extrapolation.
- Using the updated HFLAV-21 BFs, the number is 39.83 ± 0.71 .
- Uncertainties on the BGL coefficients certainly improves the lattice data. No issue with unitarity as well.

CHARGED RH CURRENT SEARCH

- Heavy RH W^- boson: deviation from pure ($V - A$) structure.
- Parameterization: $h_V \rightarrow h_{V,SM}(1 + \varepsilon_R)$. Axial FF's unchanged.
- Smoking gun: strong discrepancy between lattice (pure SM) and data (SM+NP) in $R_1(1)$, along with good agreement in $R_2(1)$.
- Lattice fixing the SM FF's allows ε_R searches from just the shape (independent of $|V_{cb}|$).
- BABAR +lattice fits converged, blinded.

SUMMARY AND NEXT STEPS

- *BABAR*-19 FF + $|V_{cb}|$ conclusions very robust. Survives checks from new lattice data and combined *BABAR*-lattice results most precise FFs.
- *BABAR* $B \rightarrow D$ data getting ready to be incorporated in joint $B \rightarrow D^{(*)}$ HQET fits.
- Stringent test for HQET: can adding higher order corrections allow fitting the data.

THE GENERIC 4-D PDF [PRD 92, 033013 (2015)]

- Differential rate (4-d fit pdf):

$$\frac{d\Gamma}{dq^2 d\Omega} \propto \sum_{i=1}^{14} f_i(\Omega) \Gamma_i(q^2)$$

- Transversity q^2 amplitudes:

$$H_0(q^2) \equiv h_0$$

$$H_{\{\parallel, \perp\}}(q^2) \equiv h_{\{\parallel, \perp\}} \underbrace{e^{i\delta_{\{\parallel, \perp\}}}}_{\text{NP phase}}$$

- Orthonormal angular basis:

- $Y_l^m \equiv Y_l^m(\theta_l, \chi)$
- $P_l^m \equiv \sqrt{2\pi} Y_l^m(\theta_V, 0)$

i	$f_i(\Omega)$	$\Gamma_i^{\text{tr}}(q^2)/(\mathbf{k}q^2)$
1	$P_0^0 Y_0^0$	$h_0^2 + h_{\parallel}^2 + h_{\perp}^2$
2	$P_2^0 Y_0^0$	$-\frac{1}{\sqrt{5}}(h_{\parallel}^2 + h_{\perp}^2) + \frac{2}{\sqrt{5}}h_0^2$
3	$P_0^0 Y_2^0$	$\frac{1}{2\sqrt{5}}[(h_{\parallel}^2 + h_{\perp}^2) - 2h_0^2]$
4	$P_2^0 Y_2^0$	$-\frac{1}{10}(h_{\parallel}^2 + h_{\perp}^2) - \frac{2}{5}h_0^2$
5	$P_2^1 \sqrt{2} \operatorname{Re}(Y_2^1)$	$-\frac{3}{5}h_{\parallel}h_0 \cos \delta_{\parallel}$
6	$P_2^1 \sqrt{2} \operatorname{Im}(Y_2^1)$	$\frac{3}{5}h_{\perp}h_0 \sin \delta_{\perp}$
7	$P_0^0 \sqrt{2} \operatorname{Re}(Y_2^2)$	$-\frac{3}{2\sqrt{15}}(h_{\parallel}^2 - h_{\perp}^2)$
8	$P_2^0 \sqrt{2} \operatorname{Re}(Y_2^2)$	$\frac{\sqrt{3}}{10}(h_{\parallel}^2 - h_{\perp}^2)$
9	$P_0^0 \sqrt{2} \operatorname{Im}(Y_2^2)$	$\sqrt{\frac{3}{5}}h_{\perp}h_{\parallel} \sin(\delta_{\perp} - \delta_{\parallel})$
10	$P_2^0 \sqrt{2} \operatorname{Im}(Y_2^2)$	$-\frac{\sqrt{3}}{5}h_{\perp}h_{\parallel} \sin(\delta_{\perp} - \delta_{\parallel})$
11	$P_0^0 Y_1^0$	$-\sqrt{3}h_{\perp}h_{\parallel} \cos(\delta_{\perp} - \delta_{\parallel})$
12	$P_2^0 Y_1^0$	$\frac{3}{\sqrt{15}}h_{\perp}h_{\parallel} \cos(\delta_{\perp} - \delta_{\parallel})$
13	$P_2^1 \sqrt{2} \operatorname{Re}(Y_1^1)$	$\frac{3}{\sqrt{5}}h_{\perp}h_0 \cos \delta_{\perp}$
14	$P_2^1 \sqrt{2} \operatorname{Im}(Y_1^1)$	$-\frac{3}{\sqrt{5}}h_{\parallel}h_0 \sin \delta_{\parallel}$